# PNAS
## www.pnas.org

Supplementary Information for

**Feast then Famine: Exiting the GOE and setting the stage for a billion years of environmental stability**

Malcolm S.W. Hodgskiss, Peter W. Crockford, Yongbo Peng, Boswell A. Wing, Tristan J. Horner

Malcolm S.W. Hodgskiss
Email: mswh@stanford.edu

Peter W. Crockford
Email: peter.crockford@weizmann.ac.il

**This PDF file includes:**

Supplementary text
Fig. S1 to S3
Tables S1 to S3
References for SI reference citations

**Supplementary Information Text**

**Kasegalik Formation microbarites.** Standard heavy mineral separation techniques were used on 5–10 cm thick sandstones of the Kasegalik Formation. This yielded microbarites roughly 200 µm in width, and weighing approximately 10–20 mg in total, from rock samples of 10–15 kg (~ 1 ppm). Owing to their small sample sizes, only one sample was analyzed for $\Delta^{17}O$, yielding a value of -0.16‰. $\delta^{138/134}Ba$ measurements (n = 9) covered a wide range from -0.51 to +0.16. Owing to the very large surface area to volume ratio of these microbarites compared to Costello Formation macrobarites, we regard the $\Delta^{17}O$ value of this sample as having been largely reset. The $\delta^{138/134}Ba$ values suggest a different source of Ba than that of the Costello Formation macrobarites due to their different mean value and much larger variation (mean of 0.00 ± 0.20‰ for Kasegalik Formation microbarites, compared to 0.10 ± 0.02‰ for Costello Formation macrobarites).

**The relationship of $\Delta^{17}O$ values to various measures of primary photosynthetic production.** The first links between $\Delta^{17}O$ values of tropospheric $O_2$ and the productivity of the biosphere were put forward by ref. 1. This work related $\Delta^{17}O$ values of atmospheric $O_2$ to gross biospheric production (*GBP*) as well as $\Delta^{17}O$ values of dissolved $O_2$ to gross primary production (*GPP*) in the photic zone of lakes and oceans. However, the term *GPP* can refer to fluxes of oxygen, carbon or energy (2) leading to the adoption of 'gross oxygen production' (*GOP*) by the oceanographic community when primary production was assessed through triple oxygen isotopes. Although $\Delta^{17}O$ values in practice reflect gross oxygen production, *GOP* is closely related to *GPP* through the stoichiometry of C-fixation to O-generation during oxygenic photosynthesis, albeit with important deviations due to photorespiration and the Mehler reaction [i.e., processes that can consume $O_2$ independent of C-fixation; (3)]. In fact, these processes lead *GOP* to overestimate carbon-based *GPP* (4). Similar to *GPP*, net primary production [*NPP*; the difference between gross primary production and the consequences of autotrophic respiration; (5)] suffers from an ambiguity depending on whether it is defined on the basis of carbon, oxygen, or energy fluxes. Comparison of oxygen-based measurements of *GPP* and oxygen-based and carbon-based measurements of *NPP* in the modern marine environment, display a wide range of *GPP-NPP* ratios of between 2.7-9 (4). This suggests that, although *NPP* is proportional to *GPP*, $\Delta^{17}O$-based measurements of primary production truly are gross, rather than net, monitors of photosynthetic primary production in modern marine environments. The relationships among *GPP-GOP-NPP* may be different under the variable $O_2$ production, $O_2$ consumption and atmospheric oxygen regimes that have been suggested throughout Earth history, which is an important subject of further research. In light of the significant uncertainties in many of the other control parameters relating *GOP* to $\Delta^{17}O$ values of sedimentary sulfate, as well as the current restriction of the term '*GOP*' to the oceanographic community, we choose to express our estimates of gross photosynthetic oxygen production as *GPP*, which is a term, albeit slightly more vague, but has a greater familiarity to the broad audience this study aims to target. We acknowledge however, it may be possible that, under extremely low atmospheric oxygen conditions, that the bulk of photosynthetically produced $O_2$ may be utilized for autotrophic respiration before it escapes the cell. Such a scenario would complicate the generalized relationship between *GPP, GOP,* and *NPP* drawn here, and would motivate the new investigation of how ancient $\Delta^{17}O$ measurements relate to the ancient carbon cycle.

## Methods

**Oxygen isotopes.** Oxygen isotope analyses were conducted at the Louisiana State University Oxy-Anion Stable Isotope Consortium lab. All samples were cut to remove weathered edges, and then crushed by hand in a cleaned agate mortar and pestle. In order to remove any oxygen bearing species (such as $NO_3$) that could contaminate measurements, $\sim$ 20 mg of barite sample powder was then dissolved into a 1 M sodium hydroxide (NaOH) and 0.05 M diethylenetriaminepentaacetic acid (DTPA) solution and shaken for > 12 hours (6). Samples were then filtered, acidified with double distilled 6 N HCl, and heated to 80 ˚C followed by the addition of drops of concentrated $BaCl_2$ solution that allowed samples to reprecipitate as pure barite. Samples were allowed to sit for > 12 hours followed by centrifuging and washing with deionized water three times. Barite precipitates were then dried for 24 hours. This total procedure was then repeated once more before analysis (6). Similar to ref. 7, pyrite oxidation within unpurified $BaSO_4$ samples was not calculated to be a significant enough of a contaminant to justify removal through a chromium reduction solution.

For analysis $\sim$ 10 mg of purified $BaSO_4$ was loaded onto a 316L stainless steel plate and placed in a chamber which was then flooded with $BrF_{5(g)}$. Samples were then heated with a $CO_2$ laser releasing $O_{2(g)}$ from $BaSO_{4(s)}$ with an $\sim$ 25-35% yield. Samples were then passed through a series of -196˚C cold-traps to remove impurities and then finally collected onto 5A mol-sieve at -196˚C. Samples of pure $O_{2(g)}$ were then analyzed on a Thermo MAT-253 in dual inlet mode. Repeated measurements of inter-laboratory standards yielded a maximum uncertainty (1σ) on the entire analytical procedure to be < 0.05‰. Although sample yields from lazing are not 100%, repeated tests by ref. 8 determined no significant fractionations during this process, therefore we argue measured $\Delta^{17}O$ results are reflective of original $SO_4$ values.

**Sulfur isotopes.** Sulfur isotope analyses for this study were conducted at McGill University's Stable Isotope Laboratory. Samples were crushed and $\sim$ 10 mg were placed into a Thode reduction solution (9) and then heated. This process converted $SO_{4(s)}$ to $H_2S_{(g)}$ which was then carried in a $N_{2(g)}$ stream through a chilled column and bubbled through a zinc acetate solution to convert $H_2S_{(g)}$ to $ZnS_{(s)}$. $ZnS_{(s)}$ was then converted to $Ag_2S_{(s)}$ through reaction with a $AgNO_3$ solution. $Ag_2S_{(s)}$ was dried and weighed into $\sim$ 3 mg portions for analysis. For measurements, $Ag_2S_{(s)}$ was converted to $SF_{6(g)}$ by reaction with $F_{2(g)}$ and heating. $SF_{6(g)}$ was purified through several cold traps at -196˚C and -120˚C followed by gas chromatography and measured on a Thermo MAT-253 in dual inlet mode. Estimated total error (1σ) on the total analytical procedure is < 0.1‰ for $\delta^{34}S$ and 0.01 for $\Delta^{33}S$ measurements.

**Barium isotopes.** Barium isotopic analyses were conducted in the NIRVANA laboratory at Woods Hole Oceanographic Institution. Before wet chemistry commenced, labware was acid cleaned and reagents (e.g., $Na_2CO_3$) were purified in order to eliminate non-sample sources of Ba. Following ref. 10, $\sim$ 10 mg aliquots of barite samples were reacted with the purified 1 M $Na_2CO_3$ at 90˚C for > 18 hrs, allowing for $BaSO_4$ to covert to $BaCO_3$. To ensure 100% conversion, this step was repeated 3 times. Following this step samples were rinsed with deionized water to remove any unreacted $Na_2CO_3$. $BaCO_3$ was then dissolved in 2 M double distilled HCl. Aliquots of Ba containing solution were then analyzed for their Ba concentration via inductively coupled plasma mass spectrometry (ICP-MS) on a Thermo iCap-RQ. Following ICP-MS analysis ~100 ng of Ba in solution was taken from individual samples and combined with a $^{135}Ba$-$^{136}Ba$ double spike of known concentration. Ba was purified from samples via column chromatography using cleaned (6 N HCl) AG-50W-X8 resin. Isotopic analyses were then performed using a Thermo Neptune multi-collector ICP-MS and are reported as $^{138}Ba/^{134}B$ ratios relative to NIST 3104a. Uncertainty for individual

analyses for the entire analytical procedure is < 0.03‰ (2σ). Please refer to ref. 11 for complete analytical procedures.

**Figure S1.** Evaporite minerals of the Belcher Group. **A)** Macrobarites in the Costello Formation exhibit well-developed crystal habits and are 1-4 cm in length. **B)** Silica-replaced gypsum pseudomorphs have been observed along a single stratigraphic horizon in the McLeary Formation. **C)** Silica-replaced pseudomorphs of gypsum twins and rosettes are very common in the Kasegalik Formation and range from mm-scale to cm-scale in size. **D)** Halite casts in the Kasegalik Formation occur less frequently than gypsum pseudomorphs, and range in size from approximately 1-3 cm.
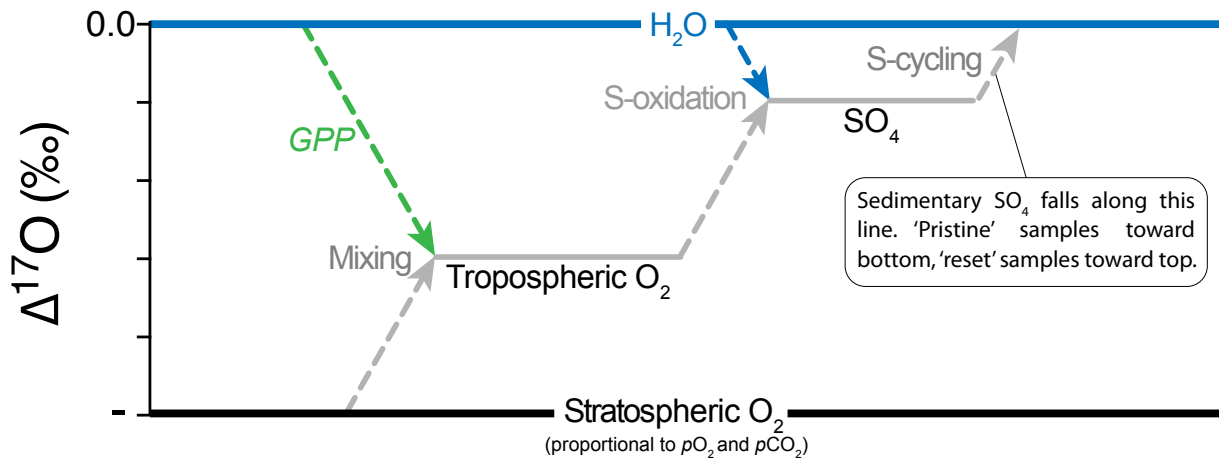
**Figure S2.** Schematic diagram of the triple oxygen ($\Delta^{17}O$) system from generation of mass independent isotope anomalies in the stratosphere to progressive dilution with oxygen from seawater through tropospheric and sedimentary reservoirs. Note that $f_{O2}$ combines both the S-oxidation and S-cycling steps in the figure.
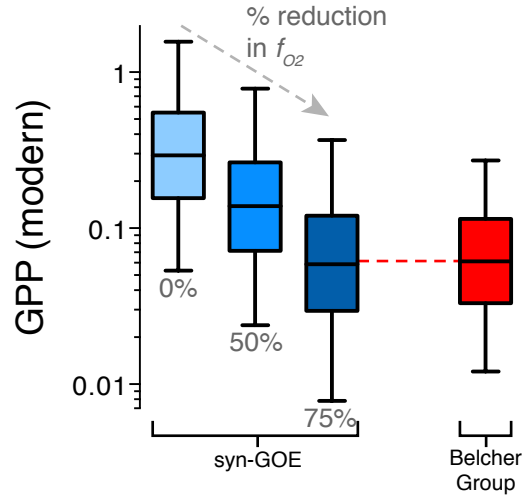
**Fig. S3.** The impacts of changing $f_{O_2}$ on *GPP* estimates. The 0% reduction in $f_{O_2}$ scenario corresponds to 8-15% of oxygen in $SO_4$ being sourced from atmospheric $O_2$. At 50%, 4-7.5% of oxygen in sulfate is from atmospheric $O_2$. At 75%, 2-3.75% of oxygen in sulfate is from atmospheric $O_2$. To explain the decrease in $\Delta^{17}O$ between syn-GOE and post-GOE samples (represented here by the Belcher Group) solely by changes in $f_{O_2}$ would require a 75% decrease of atmospheric $O_2$ incorporated into $SO_4$ from experimentally derived estimates (17).

**Table S1.** Summary of oxygen, sulfur and barium isotope results. The associated errors with analytical procedures are presented in the Methods section. Note that only one $\Delta^{17}O$ measurement, and no $\delta^{34}S$, $\Delta^{33}S$, or $\Delta^{36}S$ measurements were conducted on microbarite-bearing samples due to orders-of-magnitude less sulfate than in macrobarite samples.

| Sample type | Sample | | $\Delta^{17}O$ (‰) | $\delta^{138/134}Ba$ (‰) | $\delta^{34}S$ (‰) | $\Delta^{33}S$ (‰) | $\Delta^{36}S$ (‰) |
|---|---|---|---|---|---|---|---|
| Costello Formation Macrobarite | MB1713.103.0 | A | --- | 0.12 | 23.2 | -0.09 | 0.30 |
| | | B | -0.55 | 0.08 | 28.3 | -0.05 | 0.29 |
| | | C | -0.76 | 0.12, 0.10 | 19.6 | -0.11 | 0.19 |
| | | D | -0.64 | 0.10 | 20.1 | -0.07 | 0.20 |
| | | E | -0.78 | 0.08 | 21.4 | -0.09 | 0.27 |
| | | F | -0.68 | 0.11 | 21.4 | -0.09 | 1.05 |
| | | G | -0.70 | --- | 24.1 | -0.07 | 0.30 |
| | | H | -0.72 | --- | 23.9 | -0.09 | 0.31 |
| | | I | -0.71 | --- | 22.4 | -0.09 | 0.29 |
| Kasegalik Formation Microbarite | MB1601 | 203.6 | --- | 0.11 | --- | --- | --- |
| | | 350.2 | --- | 0.16 | --- | --- | --- |
| | | 373.9 | --- | 0.10 | --- | --- | --- |
| | | 504.6 | -0.16 | 0.06 | --- | --- | --- |
| | MB1701 | 174.7 | --- | -0.51 | --- | --- | --- |
| | | 800.0 | --- | 0.10 | --- | --- | --- |
| | | 944.0 | --- | -0.03 | --- | --- | --- |
| | MB1702 | 581.1 | --- | -0.03 | --- | --- | --- |
| | MB1703 | 139.2 | --- | 0.04 | --- | --- | --- |
| Analytical uncertainty | | | <0.05‰ (1σ) | <0.03‰ (2σ) | <0.1‰ (1σ) | <0.01‰ (1σ) | <0.2‰ (1σ) |

**Table S2. Summary of input parameters into model *GPP* calculations. Refer to Table S3 for $pO_2$ and $pCO_2$ parameters for each scenario.**

| Parameter | Value | Reference |
|---|---|---|
| $pO_2$ at 1 Pre-Anthropogenic Level (PAL) | 1 PAL = 209500 ppmv | - |
| $pCO_2$ at 1 Pre-Anthropogenic Level (PAL) | 1 PAL = 280 ppmv | - |
| Reference $pO_2$-$pCO_2$ ratio at 1 Pre-Anthropogenic Level (PAL) | 748.21 | - |
| $pCO_2$ range in calculations | 7 – 58 PAL | 12 - 14 |
| Pre-Anthropogenic $O_2$ residence time | 1244 yr | 15 |
| $\Delta^{17}O$ of modern $O_2$ using arithmetic definition for $\Delta^{17}O$ and slope of 0.5305 | -0.546‰ | 16 |
| Fraction of $O_2$ incorporation during sulfide oxidation | 0.08 – 0.15 | 17 |
| Rate constant for stratosphere-troposphere exchange | 0.0426 $yr^{-1}$ | 18-20 |
| Fraction of $O_2$ in stratospheric $O_2$-$O_3$-$CO_2$ cycles | 0.1156 | 20 |
| Reference $pO_2$-$pCO_2$ ratio in $O_2$-$O_3$-$CO_2$ isotope fractionation experiments | 1.23 | 21 |
| End-member low $pO_2/pCO_2$ ratio $\delta^{18}O_{CO2-O2}$ value in $O_2$-$O_3$-$CO_2$ isotope fractionation experiments at low $pO_2$ | 64‰ | 21 |
| End-member high $pO_2/pCO_2$ ratio $\delta^{18}O_{CO2-O2}$ value in $O_2$-$O_3$-$CO_2$ isotope fractionation experiments at low $pO_2$ | 146‰ | 21 |
| Slope to fit $\delta^{18}O_{CO2-O2}$ and $\Delta^{17}O_{CO2-O2}$ using arithmetic definition for $\Delta^{17}O$ and slope of 0.5305 | 0.5167 | 21, 22 |
| Intercept of fit to $\delta^{18}O_{CO2-O2}$ and $\Delta^{17}O_{CO2-O2}$ using arithmetic definition for $\Delta^{17}O$ and slope of 0.5305 | -8.025‰ | 21, 22 |

**Table S3. Summary of *GPP* calculation results. Refer to Table S2 for all Monte Carlo parameters other than $pO_2$ and $pCO_2$.**

| | Costello Fm | Myrtle Shale | Sibley Group | Syn-GOE | Syn-GOE | Syn-GOE |
|---|---|---|---|---|---|---|
| $pO_2$ (% modern) | 0.1 – 1.0 | 0.1 – 1.0 | 0.1 – 1.0 | 0.1 – 1.0 | 1.0 – 10.0 | 10.0 – 100.0 |
| $pCO_2$ (PAL) | 7 – 58 | 5 – 40 | 2 – 30 | 8.5 – 100 | 8.5 – 100 | 8.5 – 100 |
| Total number of values | 10000 | 10000 | 10000 | 10000 | 10000 | 10000 |
| Number of excluded values | 0 | 0 | 0 | 0 | 0 | 0 |
| Number of binned values | 10000 | 10000 | 10000 | 10000 | 10000 | 10000 |
| Minimum | 0.003 | 0.001 | -0.001 | 0 | 0.019 | 0.514 |
| 25% Percentile | 0.032 | 0.036 | 0.033 | 0.155 | 0.360 | 6.79 |
| Median | 0.060 | 0.067 | 0.062 | 0.297 | 0.618 | 11.3 |
| 75% Percentile | 0.111 | 0.124 | 0.116 | 0.564 | 1.07 | 18.2 |
| Maximum | 0.560 | 0.589 | 0.824 | 4.78 | 8.30 | 110 |
| Mean | 0.081 | 0.090 | 0.087 | 0.434 | 0.805 | 14.3 |
| Std. Deviation | 0.067 | 0.073 | 0.077 | 0.430 | 0.629 | 11.2 |
| Std. Error of Mean | 0.001 | 0.001 | 0.001 | 0.004 | 0.006 | 0.112 |
| Lower 95% CI of mean | 0.080 | 0.089 | 0.086 | 0.426 | 0.793 | 14.1 |
| Upper 95% CI of mean | 0.082 | 0.091 | 0.089 | 0.443 | 0.817 | 14.6 |

**References**

1. Luz B, et al. (1999) Triple-isotope composition of atmospheric oxygen as a tracer of biosphere productivity. *Nature* 400:547-550.
2. Nicholson D, Stanley RH, Doney SC (2014) The triple oxygen isotope tracer of primary productivity in a dynamic ocean model. *Global Biogeochem Cy* 28:538-552.
3. Bender M, et al. (1987) A comparison of four methods for determining planktonic community production. *Limnol Oceanogr* 32:1085-1098.
4. Juranek LW, Quay PD (2013) Using triple isotopes of dissolved oxygen to evaluate global marine productivity. *Ann. Rev. Mar. Sci.*, 5:503-524.
5. Sigman DM, Hain MP (2012) The biological productivity of the ocean. *Nature Ed Knowl* 3:1-16.
6. Bao H (2006) Purifying barite for oxygen isotope measurement by dissolution and reprecipitation in a chelating solution. *Anal Chem* 78:304-309.
7. Crockford PW, et al. (2016) Triple oxygen and multiple sulfur isotope constraints on the evolution of the post-Marinoan sulfur cycle. *Earth Planet Sci Lett* 435:74-83.
8. Bao H, Lyons JR, Zhou C (2008) Triple oxygen isotope evidence for elevated $CO_2$ levels after a Neoproterozoic glaciation. *Nature* 453:504-506.
9. Thode HG, Monster J, Dunford HB (1961) Sulphur isotope geochemistry. *Geochim Cosmochim Ac* 25:159-174.
10. Breit GN, Simmons EC, Goldhaber MB (1985) Dissolution of barite for the analysis of strontium isotopes and other chemical and isotopic variations using aqueous sodium carbonate. *Chem Geol* 52:333-336.
11. Horner TJ, Kinsley CW, Nielsen SG (2015) Barium-isotopic fractionation in seawater mediated by barite cycling and oceanic circulation. *Earth Planet Sci Lett* 430:511-522.
12. Wolf ET, Toon OB (2013) Hospitable Archean climates simulated by a general circulation model. *Astrobiology* 13:656-673.
13. Wiggering H, Beukes NJ (1990) Petrography and geochemistry of a 2000–2200-Ma-old hematitic paleo-alteration profile on Ongeluk basalt of the Transvaal Supergroup, Griqualand West, South Africa. *Precam. Res.* 46:241-258.
14. Sheldon ND (2006) Precambrian paleosols and atmospheric $CO_2$ levels. *Precam. Res.* 147:148-155.
15. Bender M, Sowers T, Labeyrie L (1994) The Dole effect and its variations during the last 130,000 years as measured in the Vostok ice core. *Global Biogeochem. Cyc.* 8:363-376.
16. Hayles JA, Cao X, Bao H (2017) The statistical mechanical basis of the triple isotope fractionation relationship. *Geochem Perspect Lett* 3:1-11.
17. Balci N, Shanks WC, Mayer B, Mandernack KW (2007) Oxygen and sulfur isotope systematics of sulfate produced by bacterial and abiotic oxidation of pyrite. *Geochim Cosmochim Ac* 71:3796-3811.
18. Linz M, et al. (2017) The strength of the meridional overturning circulation of the stratosphere. *Nat. Geosci.* 10:663–667.
19. Trenberth K, Smith EL (2005) The mass of the atmosphere: a constraint on global analyses. *J. Clim.* 18:864–875.
20. Crockford PW, et al. (2018) Triple oxygen isotope evidence for limited mid-Proterozoic primary productivity. *Nature* 559:613-616.
21. Shaheen R, Janssen C, Röckmann T (2007) Investigations of the photochemical isotope equilibrium between $O_2$, $CO_2$ and $O_3$. *Atm. Chem. and Phys.* 7:495-509.
22. Cao X, Bao H (2013) Dynamic model constraints on oxygen-17 depletion in atmospheric $O_2$ after a snowball Earth. *Proc Natl Acad Sci USA* 110:14546-14550.